Available online at http://ijcpe.uobaghdad.edu.iq and www.iasj.net
Iraqi Journal of Chemical and Petroleum Engineering
Vol. 24 No.3 (September 2023) 55 – 68
EISSN: 2618-0707, PISSN: 1997-4884

Petrophysical Analysis Based on Well Logging Data for Tight Carbonate Reservoir: The SADI Formation Case in Halfaya Oil Field

Safiyya A. Jassam [a, *], Omar AL-Fatlawi [a, b], and Celal Hakan Canbaz [c]

a Petroleum Engineering Department, College of Engineering, University of Baghdad, Baghdad, Iraq
b Curtin University, WA School of Mines, Mineral and Chemical Engineering, Kensington, Australia
c Climpach Consultancy, İzmir, Turkey

Abstract

Carbonate reservoirs are an essential source of hydrocarbons worldwide, and their petrophysical properties play a crucial role in hydrocarbon production. Carbonate reservoirs' most critical petrophysical properties are porosity, permeability, and water saturation. A tight reservoir refers to a reservoir with low porosity and permeability, which means it is difficult for fluids to move from one side to another. This study's primary goal is to evaluate reservoir properties and lithological identification of the SADI Formation in the Halfaya oil field. It is considered one of Iraq's most significant oilfields, 35 km south of Amarah. The Sadi formation consists of four units: A, B1, B2, and B3. Sadi A was excluded as it was not filled with hydrocarbons. The structural and petrophysical models were built based on data gathered from five oil wells. The data from the available well logs, including RHOB, NPHI, SONIC, Gamma-ray, Caliper, and resistivity logs, was used to calculate the petrophysical properties. These logs were analyzed and corrected for environmental factors using IP V3.5 software. where the average formation water resistivity (R_w = 0.04), average mud filtrate resistivity (R_{mf} = 0.06), and Archie's parameters (m = 2, n = 1.9, and a = 1) were determined. The well-log data values calculated the porosity, permeability, water saturation, and net-to-gross thickness ratio (N/G).

Keywords: Petrophysical properties, Carbonate reservoirs, formation evaluation, (Flow Zone Indicator) FZI.

Received on 03/10/2022, Received in Revised Form on 23/11/2022, Accepted on 24/11/2022, Published on 30/09/2023

https://doi.org/10.31699/IJCPE.2023.3.6

1- Introduction

Carbonate reservoirs are an essential source of hydrocarbons worldwide, and their petrophysical properties play a crucial role in hydrocarbon production [1-3]. Porosity, permeability, and saturation are the carbonate reservoir's most important petrophysical properties [4-6]. Tight carbonate reservoirs typically have porosities of less than 10% and permeabilities of less than 0.1 MD [7]. Tight carbonate reservoirs with low porosities and permeabilities make it challenging to produce hydrocarbons from these reservoirs [8-10]. One of the pressing challenges in petroleum applied research is the characterization of reservoirs [11, 12]. The reservoir's flow and fluid recovery behavior are influenced by significant reservoir characteristics, including water saturation, permeability, and porosity [13, 14]. Porosity and permeability in reservoirs are influenced by various factors such as rock fabric, lithology, diagenesis, and environmental settings [15, 16]. The prediction of porosity and permeability in carbonate reservoirs is crucial for reservoir evaluation and modeling [3, 17-20]. Even though the porosity classification relies on outward appearances that may or may not be connected to a specific formation process, the type of rock is based on its fundamental characteristics, and conclusions about depositional environments can be drawn from the classification of rocks [21, 22]. Without considering the method of conception through porosity categories, it is impossible to determine the porosity's formation environment, when it was modified, or even which genetic pore sorts have the most significant permeability. Identifying and explaining the correspondence between the pore characteristics of the rock matrix and those of the rock matrix and the genetic and temporal relationships between them are necessary for a thorough description of the reservoir [23-25]. Core samples are used to evaluate porosity directly, and some types of borehole logs are used to measure it indirectly. According to Darcy's porous-media equation, permeability is determined by the proportionality coefficient. The benchmark for many reservoir quality rankings is derived directly from core samples. So, a reservoir's porosity, permeability, and saturation depend on how well it can transmit fluids [26-28]. Analyzing measurements from inside the wellbore, such as cores, fluid properties measured in a lab, and well logs, to assess wells for potential hydrocarbon-bearing rocks is known as formation evaluation [29-32]. Well logs are an essential source of information for the geological

*Corresponding Author: Name: Safiyya A. Jassam, Email: jassam2008m@coeng.uobaghdad.edu.iq

and petrophysical properties of reservoir formations [33-35].

According to this study, the Sadi Formation, which was first identified by Owen and Nasr (1958) [36] from the southern Iraqi well Zubair-3, where the Sadi Formation overlies the Tanuma Formation, is the youngest, thickest, and most widespread formation of the Santonian-Campanian Sequence in the Late Cretaceous. Packstone is very common in the Sadi Formation, which consists of chalky, argillaceous, and globigerina limestones with a well-developed marl bed at the top [36]. The Sadi formation was developed in the Late Cretaceous, as shown in Fig. 1. It was divided into two sublayers according to the variation in reservoir properties: Sadi A and Sadi B. It is 124 meters thick. Sadi A consists of mud lime and has no hydrocarbons. Sadi B is oil-bearing with an average thickness of 75 m [37]. The majority of the limestone in the Sadi Formation is anticline. The Sadi reservoir has low to extra-low permeability, about less than 0.01 MD, while its porosity ranges from very poor to excellent, from 8% to 21% [38].

The SADI Formation / Halfaya oil field in Iraq poses a significant challenge for hydrocarbon production due to its complex petrophysical properties. The low porosity and permeability of tight carbonate reservoirs like Sadi B make it difficult to recover hydrocarbons efficiently [39]. The characterization of these reservoirs, which includes critical attributes such as water saturation, permeability, and porosity, is essential for reservoir modeling and evaluation.

This study addresses these challenges by utilizing well log data from five oil wells in the Halfaya oil field. Through advanced analysis and corrections for environmental factors, we have determined key parameters such as formation water resistivity, mud filtrate resistivity, and Archie's parameters. These data allow us to estimate petrophysical properties, including porosity, permeability, water saturation, and net-to-gross thickness ratio, which are critical for optimizing hydrocarbon production from the SADI Formation. This research contributes valuable insights to the field of formation evaluation and provides a deeper understanding of carbonate reservoirs. It paves the way for more effective oilfield management and development in the future.

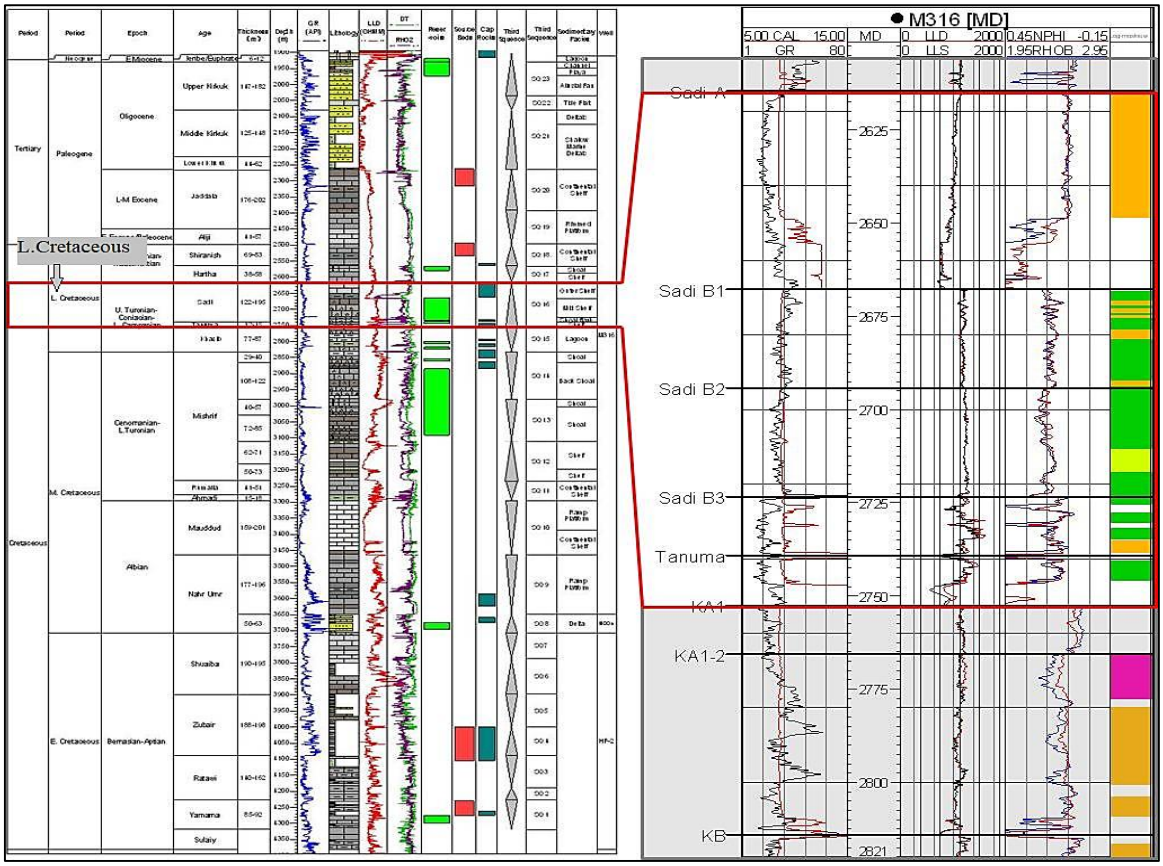

Fig. 1. Stratigraphy and Logging Characteristics of Sadi Formation [37]

2- Materials and Methods

- Well-log data

Logging the contents of drilled wells is crucial for reconstructing the various geological frameworks of an investigation area [40]. The lithology, the depth distribution of fractures, and the fundamental physical parameters (temperature, pressure, gamma, neutron, resistivity, etc.) can all be found through the logging process of a well [41, 42]. Well-logging interpretation requires specialized software for digitizing and visualizing well data [43, 44]. Well-data arrangement:

building a 2D or 3D profile or model, the oil and gas industry, and similar fields require well-data interpretation [45, 46]. Interactive Petrophysics software v3.5, interactive software for interpreting and correcting log readings for borehole environment and invasion effects, was used for the readings and corrections. The available well logs (including GR, SP, Neutron porosity NPHI, RHOB bulk density, etc.).

a. Environmental corrections of well logs

Some downhole conditions, such as salinity, drilling mud, filter cake, and borehole size, can affect the well logs and thus necessitate correction using environmental correction software [47]. The Interactive Petrophysics software, which provides an environment correction module that uses Schlumberger-produced algorithms, performed all environment corrections. The gamma-ray, density, neutron, and resistivity logs were changed to account for the effects of the size of the borehole, the salinity, the drilling mud, and the filter cake [48]. Log headers were used to obtain the information required for the corrections, such as R_{mf}, R_{mc}, and bit size. An output sample of environmental modification is shown in Fig. 2.

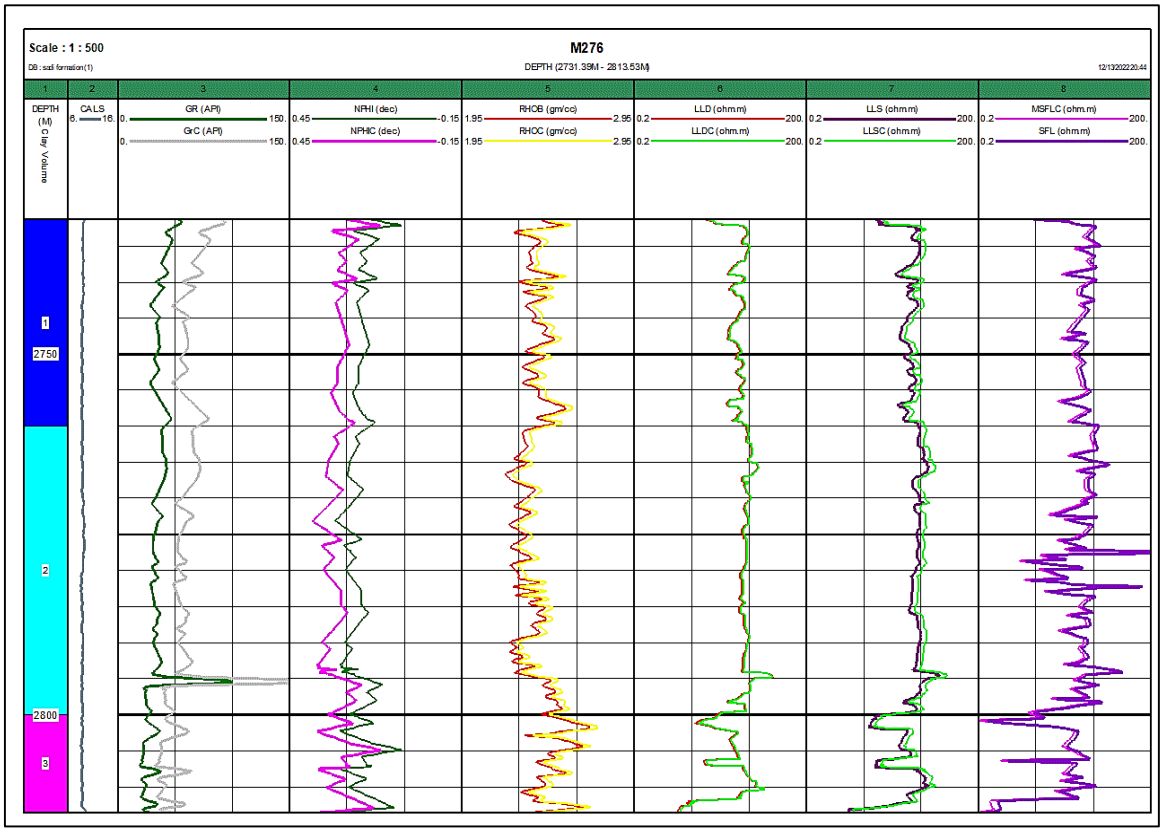

Fig. 2. Well Log Environmental Corrections Results from the Sadi Formation in Well HF001-M276

b. Porosity calculation

Porosity is an essential property of rocks that measures how much space they have that could be used to store hydrocarbons. Porosity is equal to the pore volume divided by the bulk volume.

$$Porosity = \frac{pore\ volume}{Bulk\ volumr} = \frac{Bulk\ volume - Mineral\ volume}{Bulk\ volume} \quad (1)$$

Engineers calculate fractional porosity. However, geologists frequently use a percentage to express porosity (porosity x 100). Effective porosity and "connected" pore space are the porosity that best facilitates fluid flow. Porosity is a scalar quantity because it is the bulk volume to evaluate sample size. Visual techniques and laboratory tests are used to determine porosity—for instance, the more obvious pore space. Porosity is frequently calculated throughout reduced microscope examination of core slabs. The Archie 1952 classification provides a method for determining total porosity based on visible and textural criteria. Visible porosity can be calculated through thin-section porosity estimation or image analysis equations to determine pore space through thin-section photos [49, 50]. Visual estimates can be off without point counts [51, 52]. Visual estimates of porosity through thin-section photos can be less accurate compared to point counts, which are considered the gold standard for measuring porosity [53].

The rock's porosity can be determined using neutron, formation density, and sonic logs. The lithology, pore fluid composition, and shaliness of the rock are a few other variables besides porosity that might alter these logs. Merging logs is a reliable method for determining porosity. The characteristics of the formation close to the borehole determine this equipment's readings. The sonic log isn't the best place to conduct in-depth research.

Neutron and density logs typically show notable changes within the flushed zone, though the precise depth at which this occurs depends on the porosity [54, 55]. See Table 1 and Table 2 for ways to estimate each parameter's porosity and proposed fluid and matrix properties. Also, Fig. 3. Shows the methods to estimate the porosity logs.

Table 1. Porosity Estimates based on Logs Are Summarized [56]

Logs	Required Data	Formula
Density(RHOB)	ρ_{ma}, ρ_f, ρ_b matrix, fluid, and log density	$\varphi = \frac{\rho_{ma} - \rho_b}{\rho_{ma} - \rho_f}$
Neutron(NPHI)	NPHIφ	$\varphi = \frac{\varphi_N - \varphi_{N.ma}}{\varphi_{N,f} - \varphi_{N,ma}}$
Sonic(DT)	$\triangle t_{ma}$,$\triangle t_f$ matrix, and fluid transit time	$\varphi = \frac{\triangle tma - \triangle t}{\triangle tma - \triangle t_f}$

- Effective Porosity (PHIE)

As stated by Dodge et al. (1996), engineers frequently refer to the interconnected pore volume of the rock when defining effective porosity. The effective porosity equals the total porosity minus any water dissolved in the rock's clay minerals [57].

$$\varphi_{eff} = \varphi_t * (1 - V_{Sh}) \quad (2)$$

Table 2. Proposed Fluid and Matrix Properties [56]

Parameters values	Lithology, fluid
ρ_{ma} = 2.71 g/cm^3 ρ_f = 1 g/cm3 for freshwater ($\varphi_{N,ma}$, $\varphi_{N,f}$) = 0 $\triangle$tma = 47.5 µsec/ft $\triangle t_f$ = 189 µsec/ft for freshwater	Limestone

- Total porosity (PHIT)

Total porosity(φ_t) is defined as the ratio of the volume of all pores to the bulk volume of a material. With neutron and density logs, the following equation could be used to figure out the total porosity [58]:

$$\varphi_t = \frac{\varphi_N + \varphi_D}{2} \quad (3)$$

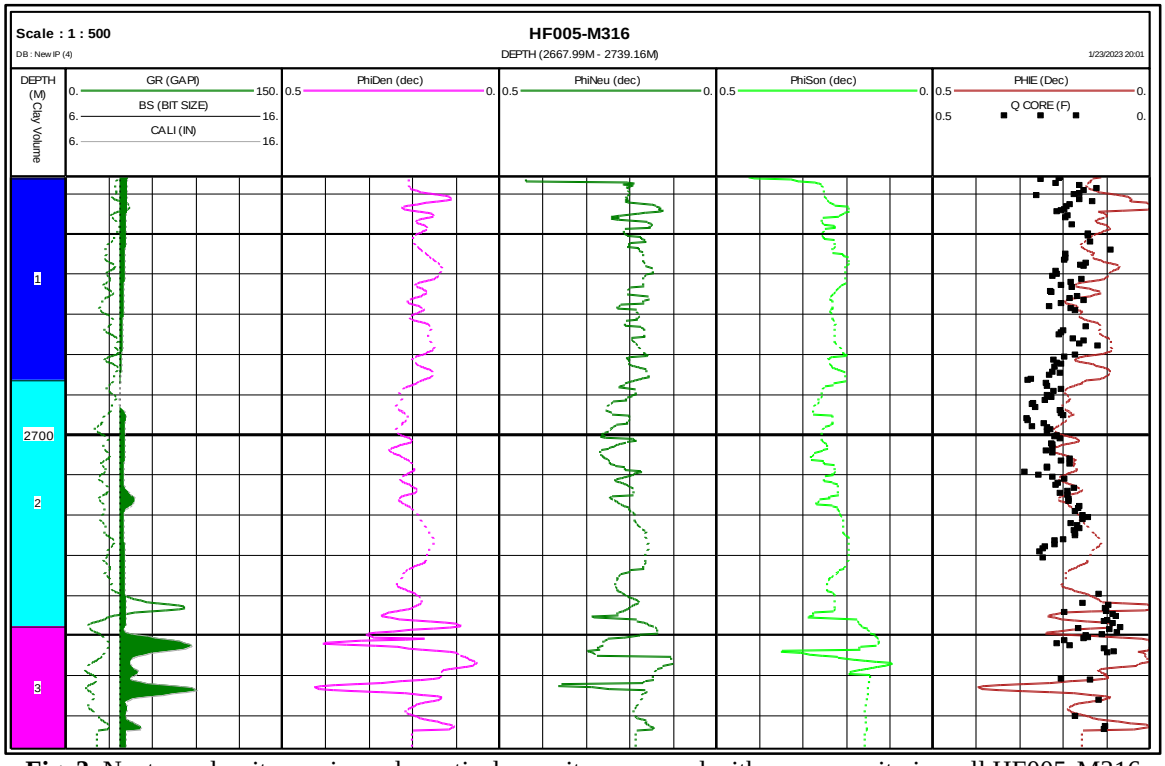

Fig. 3. Neutron, density, sonic, and practical porosity compared with core porosity in well HF005-M316

c. Permeability Prediction

Permeability is a term used to describe a rock's ability to allow fluids to pass through it. Darcy's law for flow through a porous medium is as follows:

$$Q = KA \triangle p/\mu L \quad (4)$$

In this case, Q represents the rate at which a fluid with viscosity flows through a body with dimensions L and A and a pressure gradient p. For laminar flow, we can define the permeability, k, using Darcy's relation, which is as follows [56]:

$$K = q\mu L/A \triangle p \quad (5)$$

Log-derived permeability formulas for formation permeability estimates call for an infinite water saturation

(Schlumberger-1977). At any time, possible, a geologist should compare the permeability values of close production wells to the same formation when evaluating a formation utilizing log-derived permeability equations. Estimating productivity from log-derived permeabilities requires comparing the evaluated formation to wells in the area with good and bad production histories. To compare permeabilities measured in different wells, a geologist does not use an absolute value for the permeability from the log [59].
Several methods are used for permeability calculation:

- Classical method

It is one of the most famous methods of predicting permeability. The classical method can be defined as finding a mathematical relationship between core porosity and core permeability, then applying this formula to the uncored sections using the log porosity as input to obtain permeability.

The general expression for the permeability-porosity correlation is usually expressed as [59]:

$$log\ K\ =\ a\varphi\ +\ b \tag{6}$$

Where: K = permeability, MD. φ = porosity. a and b = constants to be determined for each case.

To determine the constants a and b, a cross plot is made between porosity on the x-axis versus the logarithm of permeability on the y-axis, as Eq. 6 shows a liner relationship between these parameters, with a as the slop and b as the intersect.

- Empirical Method

The second method was determining the log's permeability through three processes (Timur, Morris, and Schlumberger). The 'Timur,' 'Morris Biggs oil,' and defaults come from the Western Atlas chart book, while the 'Schlumberger Chart K3' is from the Schlumberger chart book. These equations are applied only over zones at irreducible water saturation, i.e., hydrocarbon zones above the transition zone. Eq. 7 can be used to calculate the permeability from the log (Timur, Morris, and Schlumberger), where a, b, and c are constant. Fig. 4 shows the results of this method [60]:

$$K\ =a\ (Phi^{b}/SW^{c}) \tag{7}$$

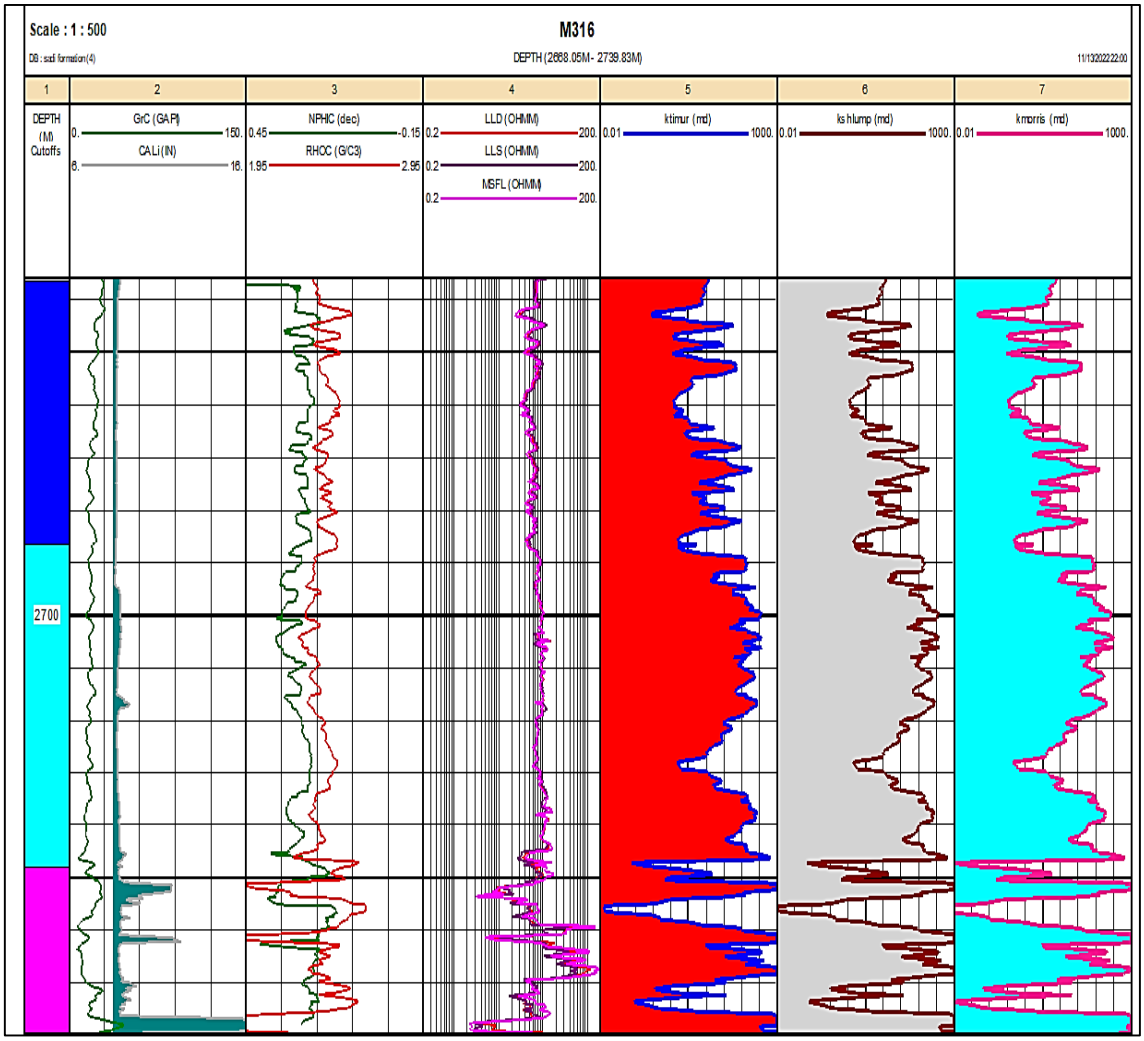

Fig. 4. Permeability Estimation from the Well Log for Well HF005-M316

- Flow Zone Indictor (FZI) Methods

The FZI method is the third method to measure permeability. Flow zone indicator depends on the geological characteristics of the material and various pore geometry of a rock mass; hence, it is a suitable parameter for determining hydraulic flow unit. High-productive zones, low-quality rocks, and diagenesis effects can be identified by a flow zone indicator (FZI) [61-63]. FZI is estimated from core data within the cored wells, and it's sometimes applied to un-cored wells through correlations with log attributes. The final approach is given influent equations:

$$RQI = 0.0314\sqrt{\frac{K}{\varphi}} \quad (8)$$

$$\varphi z \ = PHIz = (\frac{\varphi}{1-\varphi}) \quad (9)$$

$$FZI = (\frac{RQI}{\varphi z}) \quad (10)$$

By taking the logarithm of both side of Eq. 11, the final approach can be written as follow:

$$\text{Log RQI} = \text{Log FZI} + \text{Log } \varphi z \quad (11)$$

The above equation represents the straight line on the log-log plot of RQI vs. φ_z. The intercept of the straight line at φ_z=1 is each group's specific flow zone indicator. Other FZI values of core samples will show on different lines. Points that lie on each straight line got the same pore throat description and, therefore, the same flow unit. Sadi formation was divided into four FZI, and four porosity-permeability relations are applied by different equations with decisive correlated factors for each one, as in Fig. 5 and Fig. 6; the equation results of the regression analysis for the hydraulic flow units are given in Table 3.

Table 3. FZI Permeability Formula for Sadi Formation

FZI	Formula	R^2
FZI=1	K= φ^3 * (0.037 / (0.0314 * (1.0- φ)))^2	0.6789
FZI=2	K= φ^3 * (0.064 / (0.0314 * (1.0-φ)))^2	0.7485
FZI=3	K= φ^3 * (0.139 / (0.0314 * (1.0-φ)))^2	0.8473
FZI=4	K= φ^3 * (0.41 / (0.0314 * (1.0-φ)))^2	0.9056

d. Water Saturation Estimation

One of the primary inputs for evaluating hydrocarbon reserves is the calculated water saturation obtained from open-hole resistivity measurements [64]. The water saturation level is calculated using a model called Archie's equation. Since the Archie equation's parameters depend highly on carbonate characteristics, applying them in carbonate reservoirs is challenging. These findings highlight the importance of precise measurement of a, m, and n in core samples to obtain representative a, m, and n values, significantly affecting the water saturation values. Archie proposed in 1942 that there is a relationship between a rock's porosity, the amount of water it holds, and its resistivity R_t. See Fig. 7.

$$S_W^n = \frac{aR_W}{\varphi^m R_t} = R_O/R_t \quad (12)$$

Then, he explains the resistivity of rock that is completely 100% saturated with brine and how it relates to the resistivity of brine [56]. The value of rock resistivity can be expressed as a function of formation factors using the formula [56]:

$$R_O = F/R_W \quad (13)$$

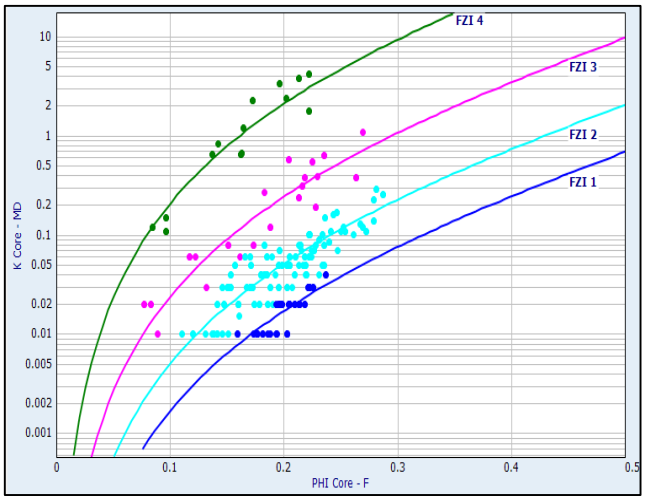

Fig. 5. Permeability vs. Porosity Cross Plot for Specific FZI

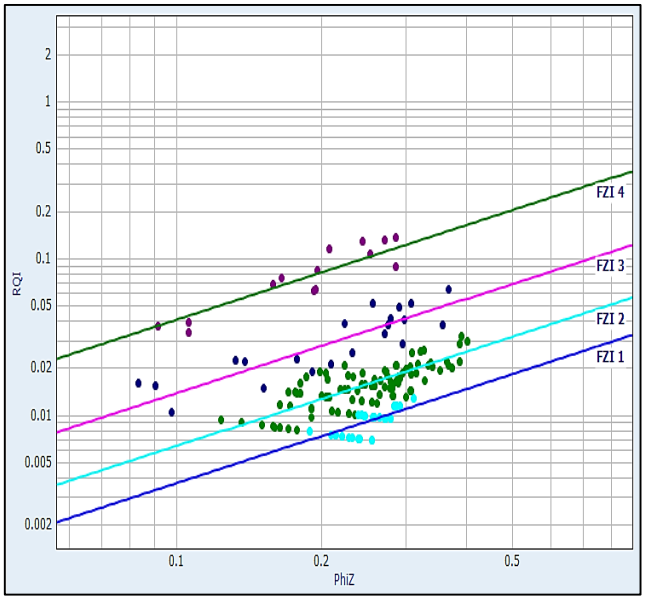

Fig. 6. RQI versus. Phiz Cross Plot

e. Shale Volume

Although shale is typically more radioactive than sand and carbonate, the amount of shale in porous reservoirs could be calculated using gamma rays. V_{shale} denotes the shale volume like a decimal percentage or fraction. This value can then be applied to sandy shale formations to evaluate them. The gamma-ray index from a gamma-ray log (VCLGR), Neutron(VCLN), and Neutron-Density

(VCLND) is used to determine the shale volume by Eq. 14 [65] and shown in Fig. 8:

$$V_{shale} = \frac{GR_{log} - GR_{min}}{GR_{max} - G_{min}} \quad (14)$$

Where: GR_{log}: Gamma-ray reading of the formation. GR_{min}: Minimum Gamma-ray. GR_{max}: Maximum Gamma-ray.

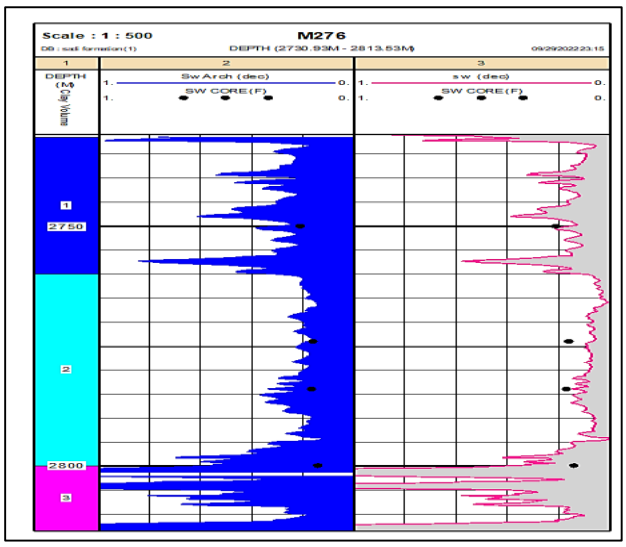

Fig. 7. Water Saturation Log Plot in Well HF001-M276

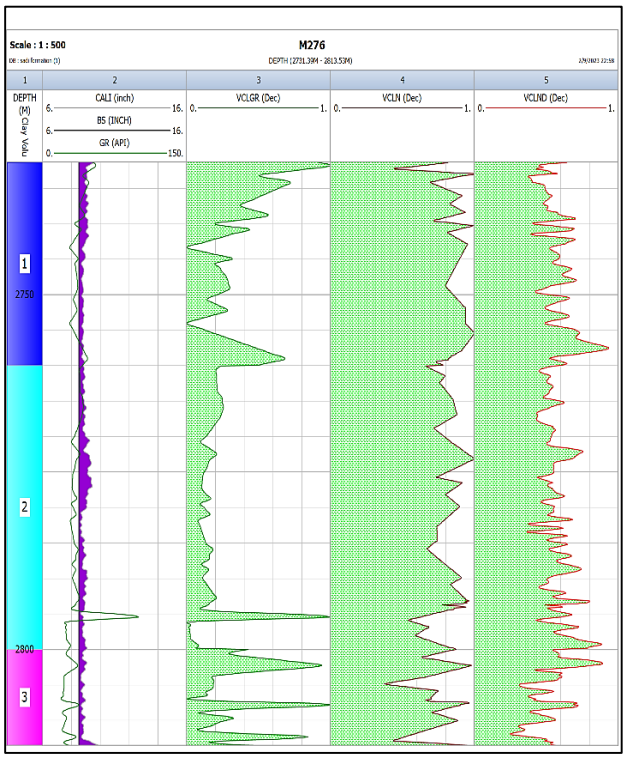

Fig. 8. Shale Volume for Well HF001-M276

3- Results

3.1. Cut-off estimation

The selection of petrophysical cutoffs for calculating net pay has been a significant source of uncertainty in earlier methods. Traditionally, a shale volume fraction (V_{shc}) cutoff is used to determine net sand, followed by applying a porosity cutoff to define the net reservoir. Finally, the cutoff is used to determine net pay and water saturation (S_w) in the net reservoir [66]. Cutoffs must be carefully chosen to ensure that the hydrocarbons excluded are truly unproducible.

a. Porosity Cut-off

The core porosity cutoff was established by analyzing the data at hand. To do so, a plot was selected in which "permeability (log scale) vs. porosity (linear scale) with the best-fit line intersecting a straight line at a permeability value of (0.01 MD). The porosity cutoffs for the Sadi B1 and B2 units and Sadi B3 units are 12% and 10%, respectively. Fig. 9 and Fig. 10 show the relationship between the core permeability vs. core Porosity to find cut-off porosity in Sadi B1, B2 and B3 units.

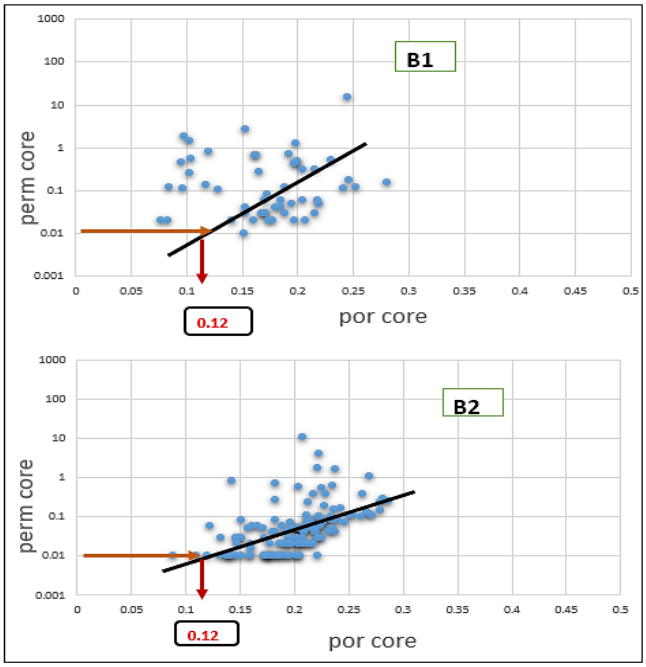

Fig. 9. Core Permeability vs. Core Porosity to Find Cut-off Porosity in Sadi B1and B2 Units

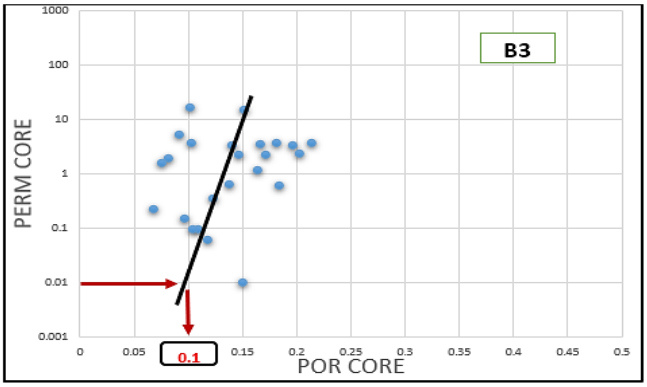

Fig. 10. Core Permeability vs. Core Porosity to Find Cut-off Porosity in Sadi B3 Unit

b. The water saturation cut-off

We determined the water saturation cut-off values for the Sadi formation reservoir units by drawing a cross plot between water saturation and log porosity. Then, we used the point where the log porosity cut-off value and the drawn curve intersected as a criterion. All units in the Sadi formation have a 50% water saturation cutoff. Fig. 11 and Fig. 12 show the water saturation cut-off for three Sadi units.

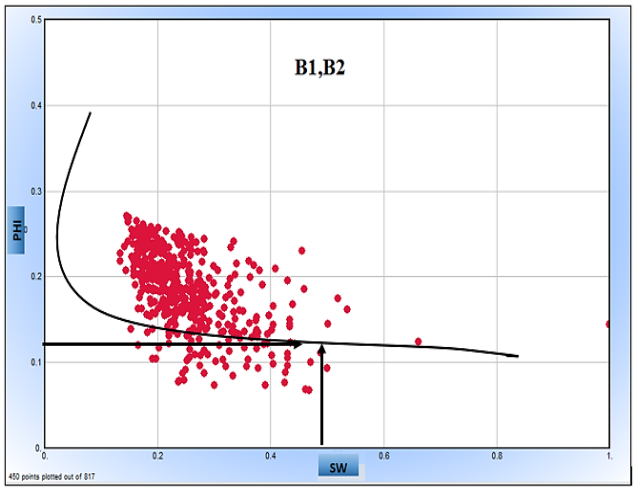

Fig. 11. Log Porosity vs. Water Saturation in Sadi B1and B2 Units

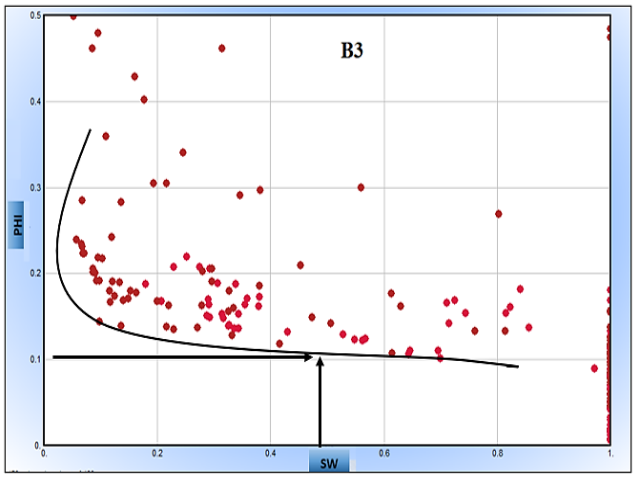

Fig. 12. Log Porosity vs. Water Saturation in Sadi B3 Unit

c. Shale Volume cut-off

By constructing a plot of log porosity vs. shale volume for reservoir units in the Sadi formation, cut-off values for shale volume were determined. Then, the shale volume cut-off value was found where this curve met the log porosity cut-off value. All Sadi formation units have a cut-off for the amount of shale at 25%.

3.2. Net-To-Gross (NTG)

The net-to-gross ratio measures the thickness of productive (net) reservoir rock compared to the thickness of the entire reservoir (gross) [67]. This term describes the reservoir areas that can be used to get hydrocarbons. Researchers' most common parameters are φ, V_{sh}, S_w, and k [68]. Cut-offs for porosity, permeability, and water saturation have been used to calculate net-to-gross ratios for the Sadi formation, along with the cut-offs. A net-to-gross pay thickness is the thickness of pay zones relative to reservoirs. The term "net pay" refers to the depth of the porous and permeable zones that contain economically viable amounts of hydrocarbons, as shown in Fig. 13. The results show that the Sadi A region, which is in the upper part of the chart, does not have any hydrocarbons, so it did not contain any results. As for the other three layers, B1, B2, and B3 are suitable oil reservoirs. Fig. 14 shows an example of converting NTG thickness for well HF001-M276.

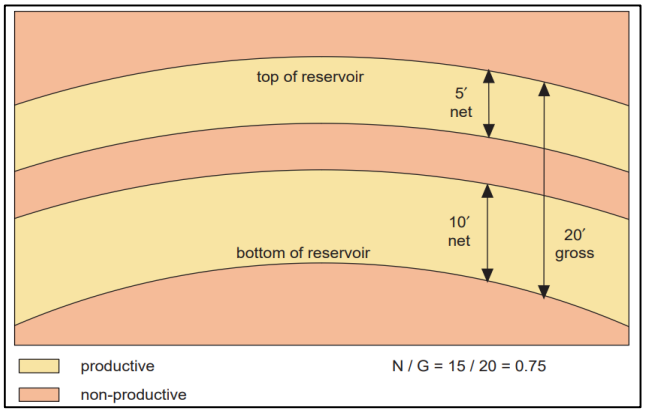

Fig. 13. Net-To-Gross Ratio [28]

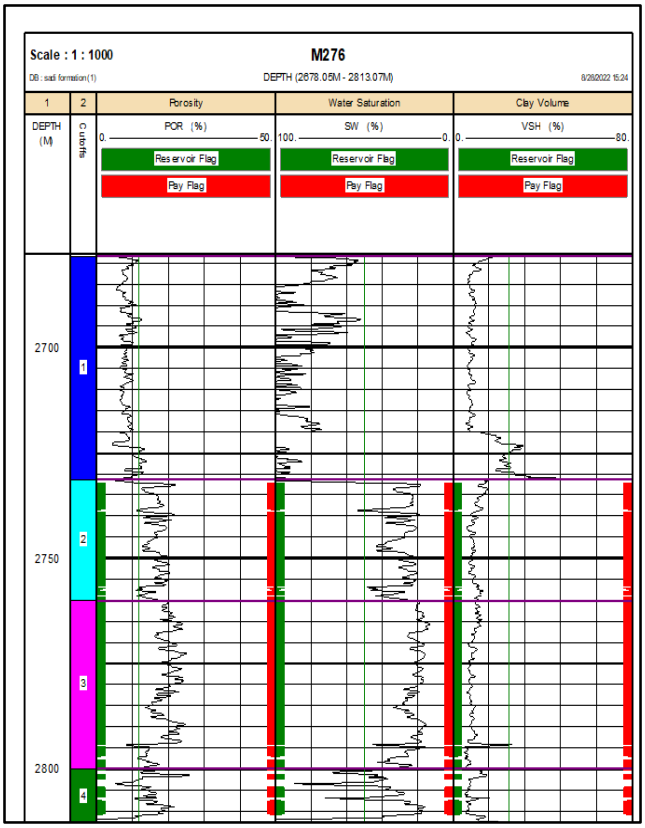

Fig. 14. Shows an Example of Converting N/G Thickness for Well HF001-M276

3.3. Lithology Identification

a. Neutron-density cross plot

The lithology of the Sadi formations is primarily limestone porous, with calcite as the main mineral content; this result is consistent with the geological reports from the wells [69], which identify the Sadi formation as limestone porous with some dolomite, as seen and inferred from the description by the two types of cross-plots. The first cross-plot to determine lithology is Neutron porosity (PhiNeu)-Density, based on density and neutron porosity logs. Fig. 15 and Fig. 16 show the different lithologies of Sadi from Logging Interpretation.

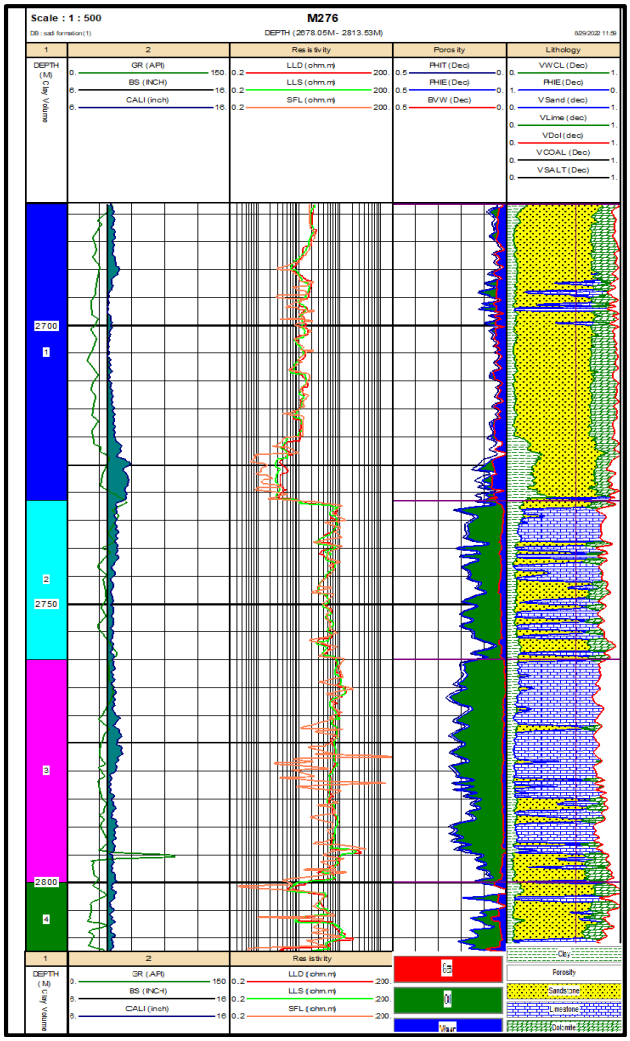

Fig. 15. Comprehensive Lithology of Sadi from Logging Interpretation, Well HF001-M276

b. M-N cross plot

The lithology-dependent variables M and N must be calculated for the sonic, neutron, and density log, which are all required for the M-N plot. Matrix porosity has little effect on M and N values (inter-granular and intercrystalline). Lithology is more pronounced when these two variables are plotted crosswise. Fig. 17 shows the M-N cross plot, and the following equations are used to calculate the values of M and N. [59]:

$$M = ((\Delta t_{fluid} - \Delta t_{log}))/\,(\rho_{bulk} - \rho_{fluid}) \times 0.01 \quad (15)$$

$$N = (\emptyset N_{fluid} - \emptyset N_{log}\,)\,/(\rho_{bulk} - \rho_{fluid}) \quad (16)$$

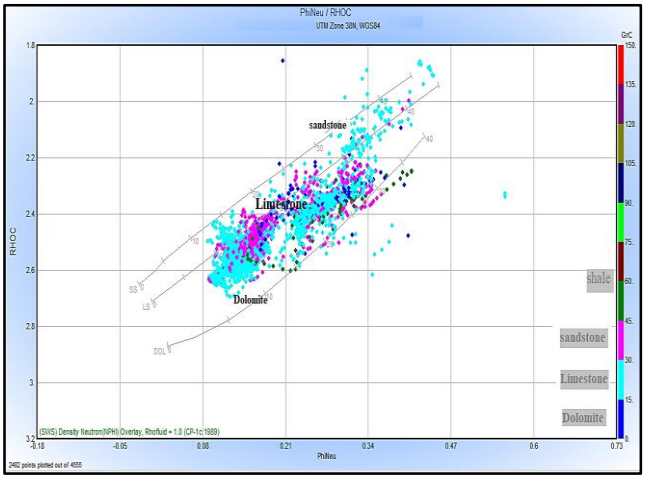

Fig. 16. Density-Neutron Lithology Cross Plot of All Wells in Sadi Reservoir (Generated by IP Software)

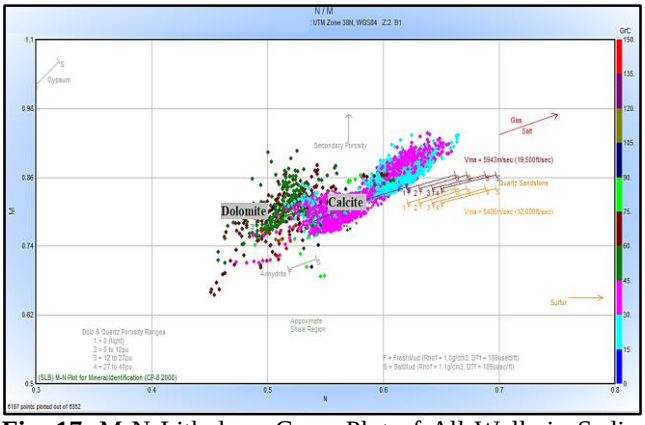

Fig. 17. M-N Lithology Cross Plot of All Wells in Sadi Reservoir (Generated by IP Software)

4- Conclusions

- The porosity determined from the core data for the two wells (M276 and M316) was compared to the porosity information inferred from the well log data for those two wells. The density porosity(PHID) was the most consistent with the porosity data from the core analyses. In contrast, the neutron porosity(NPHI) was the least compatible. This study used PHID rather than NPHID to calculate the PHIE to achieve higher accuracy.
- The permeability of uncored wells was predicted by the FZI approach, which presented the best-determined match from other methods: classical and empirical methods.
- Using the neutron-density and M-N Cross Plots, it was determined that the Sadi formation's lithology is

primarily limestone and that its significant mineral content is calcite with some dolomite.

- Cutoffs are used to define terms such as "net pay" and "reservoir rock," where the value of reservoir rock is described using a 12% cutoff for porosity and a 50% cutoff for water saturation. The 12% porosity cut-off value calculates the reservoir's net thickness. If the reservoir has less than 50% water saturation, it is deemed to contain hydrocarbons to calculate net pay. The saturation cutoff and unique core analysis can predict the relative permeability ratio. A portion of the hydrocarbons-in-place is left out of the reserves calculation to calculate net pay using cutoffs. Cutoffs must be carefully chosen to ensure that the hydrocarbons excluded are truly unproducible.
- The results show that the Sadi A region lacks hydrocarbons and thus contains no results. The other three layers, B1, B2, and B3, are suitable oil reservoirs that cover 75 m of the total area of 124 m.

Nomenclature

Nomenclature	Description
ρma	The matrix's density g/cm3
ρf	The density of fluid g/cm3
ρb	The formation fluid's density of g/cm3
SW	Water saturation fraction
Sw arch	Water saturation Archie equation fraction
Rw	formation water resistivity Ωm
Rt	The resistivity of rock Ωm
RO	The resistivity of rock Ωm
Rmf	Mud filtrate resistivity(ohm-m) Ωm
Rmc	Mudcake resistivity(ohm-m) Ωm
Q	Flow rate (m3/s)
L	Length of the sample in units [2]
A	Cross-sectional area(m2) in Darcy equation
K	Permeability coefficient(m2)
IP	Interactive Petrophysics software
IGR	Gamma-ray index
Grmin	Minimum Gamma-ray
GRmax	Maximum Gamma-ray
Grlog	Gamma-ray reading of the formation
GR	Gamma Ray
F	Formation resistivity factor
a,m,n	Archie's parameters
μ	Fluid of dynamic viscosity(pa.s)
△tma	The transit time of the matrix(μsec/ft)
$\triangle t_f$	The transit time of the formation fluid(μsec/ft)
△t	The transit time from the sonic log(μsec/ft)
RQI	The reservoir quality index (μm)
FZI	Flow Zone Indicator (μm)
HFU	Hydraulic Flow Unit

References

[1] J. Hou, L. Zhao, W. Zhao, Z. Feng, X. Wang, and X. Zeng, "Evaluation of pore-throat structures of carbonate reservoirs based on petrophysical facies division," *Frontiers in Earth Science*, vol. 11, p. 1164751, 2023, http://doi.org/10.3389/feart.2023.1164751

[2] M. Mehrad, A. Ramezanzadeh, M. Bajolvand, and M. R. Hajsaeedi, "Estimating shear wave velocity in carbonate reservoirs from petrophysical logs using intelligent algorithms," *Journal of Petroleum Science and Engineering*, vol. 212, p. 110254, 2022, https://doi.org/10.1016/j.petrol.2022.110254

[3] O. Salman, O. F. Hasan, and S. Al-Jawad, "Permeability Prediction in One of Iraqi Carbonate Reservoir Using Statistical, Hydraulic Flow Units, and ANN Methods," *Iraqi Journal of Chemical and Petroleum Engineering*, vol. 23 ,no. 4, pp. 17-24, 2022, https://doi.org/10.31699/IJCPE.2022.4.3

[4] Z. Ernando, M. Aip, T. B. Nordin, I. Alliyah, A. S. B. Johari, and F. Muhammad, "Rock Type and Generalization of Permeability-Porosity Relationship for Carbonate Reservoir in Ketapang Block, Indonesia," 2022, https://doi.org/10.29118/ipa22-g-283

[5] O. Salman, O. Al-Fatlawi, and S. Al-Jawad, "Reservoir Characterization and Rock Typing of Carbonate Reservoir in the Southeast of Iraq," *The Iraqi Geological Journal*, pp. 221-237, 2023, https://doi.org/10.46717/igj.56.1A.17ms-2023-1-29

[6] G. Zhu, X. Wang, and R. Guo, "Comprehensive Formation Evaluation of HF Carbonate Reservoir by Integrating the Static and Dynamic Parameters," in *SPE Asia Pacific Oil and Gas Conference and Exhibition*, 2013: OnePetro, https://doi.org/10.2118/165896-MS

[7] O. F. Al-Fatlawi, "Numerical simulation for the reserve estimation and production optimization from tight gas reservoirs," Curtin University, 2018.

[8] O. Al-Fatlawi, M. M. Hossain, and A. Saeedi, "A new practical method for predicting equivalent drainage area of well in tight gas reservoirs," in *SPE Europec featured at EAGE Conference and Exhibition?*, 2017: SPE, p. D031S007R007, https://doi.org/10.2118/185854-MS

[9] A. Cardona and J. C. Santamarina, "Carbonate rocks: Matrix permeability estimation," *AAPG Bulletin*, vol. 104, no. 1, pp. 131-144, 2020, https://doi.org/10.1306/05021917345

[10] O. Al-Fatlawi, M. H. Mofazzal, S. Hicks, and A. Saeedi, "Developed material balance approach for estimating gas initially in place and ultimate recovery for tight gas reservoirs," in *Abu Dhabi International Petroleum Exhibition & Conference*, 2016: OnePetro, https://doi.org/10.2118/183015-MS

[11] I. Shishkova *et al.*, "Challenges in petroleum characterization—A review," *Energies* ,vol. 15, no. 20, p. 7765, 2022, https://doi.org/10.3390/en15207765

[12] F. A. Anifowose, J. Labadin, and A. Abdulraheem, "Hybrid intelligent systems in petroleum reservoir characterization and modeling: the journey so far and the challenges ahead," *Journal of Petroleum Exploration and Production Technology*, vol. 7, pp. 251-263, 2017, https://doi.org/10.1007/S13202-016-0257-3

[13] S. M. Awadh, H. S. Al-Mimar, and Z. M. Yaseen, "Effect of water flooding on oil reservoir permeability: saturation index prediction model for giant oil reservoirs, Southern Iraq," *Natural Resources Research*, vol. 30, no. 6, pp. 4403-4415, 2021, https://doi.org/10.1007/S11053-021-09923-4

[14] R. Rahimi, M. Bagheri, and M. Masihi, "Characterization and estimation of reservoir properties in a carbonate reservoir in Southern Iran by fractal methods," *Journal of Petroleum Exploration and Production Technology*, vol. 8, pp. 31-41, 2018, https://doi.org/10.1007/s13202-017-0358-7

[15] M. S. Rosid, R. A. Kurnia, and M. W. Haidar, "Estimation of 3D Carbonate Reservoir Permeability and Interparticle Porosity Based on Rock Types Distribution Model," *GEOMATE Journal*, vol. 19, no. 74, pp. 59-65, 2020, https://doi.org/10.21660/2020.74.10910

[16] F. Male and I. J. Duncan, "Lessons for machine learning from the analysis of porosity-permeability transforms for carbonate reservoirs," *Journal of Petroleum Science and Engineering*, vol. 187, p. 106825, 2020, https://doi.org/10.1016/J.PETROL.2019.106825

[17] R. Kalule, H. A. Abderrahmane, W. Alameri, and M. Sassi, "Stacked ensemble machine learning for porosity and absolute permeability prediction of carbonate rock plugs," *Scientific Reports*, vol. 13, no. 1, p. 9855, 2023, https://doi.org/10.1038/s41598-023-36096-2

[18] M. M. Hossain, O. Al-Fatlawi, D. Brown, and M. Ajeel, "Numerical approach for the prediction of formation and hydraulic fracture properties considering elliptical flow regime in tight gas reservoirs," in *Offshore Technology Conference Asia*, 2018: OTC, p. D021S007R004, https://doi.org/10.4043/28418-MS

[19] P. Xu *et al.*, "Permeability prediction using logging data in a heterogeneous carbonate reservoir: A new self-adaptive predictor," *Geoenergy Science and Engineering*, vol. 224, p. 211635, 2023, https://doi.org/10.1016/j.geoen.2023.211635

[20] H. Khoshdel, A. Javaherian, M. R. Saberi, S. R. Varnousfaderani, and M. Shabani" ,Permeability estimation using rock physics modeling and seismic inversion in a carbonate reservoir," *Journal of Petroleum Science and Engineering*, vol. 219, p. 111128, 2022, https://doi.org/10.1016/j.petrol.2022.111128

[21] C. H. Moore and W. J. Wade, "The nature and classification of carbonate porosity," in *Developments in sedimentology*, vol. 67: Elsevier, 2013, pp. 51-65. https://doi.org/10.1016/B978-0-444-53831-4.00004-5

[22] G. D. Merletti *et al.*, "Integration of depositional, petrophysical, and petrographic facies for predicting permeability in tight gas reservoirs," *Interpretation*, vol. 5, no. 2, pp. SE29-SE41, 2017, https://doi.org/10.1190/INT-2016-0112.1

[23] S. Dasgupta, "Comprehensive lithological description, reservoir property, and pore-pressure prediction for unconventional shale reservoirs using rock physics: Midland reservoir characterization case study," in *Second International Meeting for Applied Geoscience & Energy*, 2022: Society of Exploration Geophysicists and American Association of Petroleum …, pp. 2203-2207, https://doi.org/10.1190/image2022-3750232.1

[24] Z. Xia, S. Li, Z. Liu, B. Wang, Y. Wang, and M. Xie, "Reservoir Characteristics of Epimetamorphic Rock Gas Reservoir in Pingxi Area, Qaidam Basin," in *Proceedings of the International Field Exploration and Development Conference 2018 8th*, 2020: Springer, pp, 397-409. https://doi.org/10.1007/978-981-13-7127-1_37

[25] A. Hassane, C. N. Ehirim, and T. Dagogo, "Rock physics diagnostic of Eocene Sokor-1 reservoir in Termit subbasin, Niger," *Journal of Petroleum Exploration and Production Technology*, vol. 11, no. 9, pp. 336 ,2021 ,1-3371. https://doi.org/10.1007/S13202-021-01259-2

[26] F. A. Aljuboori, J. H. Lee, K. A. Elraies, and K. D. Stephen, "Using statistical approaches in permeability prediction in highly heterogeneous carbonate reservoirs," *Carbonates and Evaporites*, vol. 36, no. 3, p. 49, 2021, https://doi.org/10.1007/S13146-021-00707-8

[27] W. M. Ahr, *Geology of carbonate reservoirs: the identification, description and characterization of hydrocarbon reservoirs in carbonate rocks*. John Wiley and Sons, 2011.

[28] H. Qanadeely, K. Al-Mulhim, and R. Amin, "Elements Influencing the Estimated Permeability from Pressure Transient Analysis in Comparison to Measured Permeability from Cores," in *International Petroleum Technology Conference*, 2020: IPTC, p. D022S140R002, https://doi.org/10.2523/IPTC-20101-MS

[29] F. Aminzadeh and S. N. Dasgupta, "Formation Evaluation," in *Developments in Petroleum Science*, vol. 60: Elsevier, 2013, pp. 93-128. https://doi.org/10.1016/B978-0-444-50662-7.00004-4

[30] M. O. Amabeoku, D. Kersey, A. A. Al-Harbi, A. R. Al-Belowi, and R. H. BinNasser, "Successful application of the key well concept to enhance formation evaluation," in *IPTC 2008: International Petroleum Technology Conference*, 2008: European Association of Geoscientists & Engineers, pp. cp-148-00186, https://doi.org/10.2523/IPTC-12579-MS

[31] A. M. Al-Heeti, O. F. Al-Fatlawi ,and M. M. Hossain, "Evaluation of the Mishrif Formation Using an Advanced Method of Interpretation," *Iraqi Journal of Chemical and Petroleum Engineering*, vol. 24, no. 2, pp. 41-51, 2023, https://doi.org/10.31699/IJCPE.2023.2.5

[32] C. Cavalleri, G. Brouwer, D. Kodri, D. Rose, and J.-B. T. Brinks, "Maximizing the value of pulsed-neutron logs: A complex case study of gas pressure assessment through casing," *Petrophysics*, vol. 61, no. 06, pp. 610-622, 2020, https://doi.org/10.30632/PJV61N6-2020A6

[33] R. Abdel Azim and A. Aljehani, "Neural Network Model for Permeability Prediction from Reservoir Well Logs," *Processes*, vol. 10, no. 12, p. 2587, 2022, https://doi.org/10.3390/pr10122587

[34] B. A. AL-Baldawi, "Hydrocarbon Reservoir Characterization Using Well Logs of Nahr Umr Formation in Kifl Oil field, Central Iraq," *Iraqi Journal of Science*, pp. 3544-3554, 2022, https://doi.org/10.24996/ijs.2022.63.8.27

[35] M. M. A.-N. Al-Nafie, S. Y. Jassim, and A. J. Al-Khafaji, "Determination of reservoir properties for Nahr Umr Formation based on core plugs ,lithofacies, and well logs in Noor oilfield, southern Iraq," *Iraqi Journal of Science*, 2022, https://doi.org/10.24996/ijs.2022.63.5.22

[36] S. Z. Jassim and J. C. Goff, *Geology of Iraq*. DOLIN, sro, distributed by Geological Society of London, 2006.

[37] Ministry of Oil - Iraq, "Development plan P2-3-Sadi-Tanuma," 2012 .

[38] A. K. Farouk and A. A. Al-haleem, "Integrating Petrophysical and Geomechanical Rock Properties for Determination of Fracability of an Iraqi Tight Oil Reservoir," *The Iraqi Geological Journal* ,pp. 81-94, 2022, https://doi.org/10.46717/igj.55.1F.7Ms-2022-06-22

[39] S. A. Jassam and O. Al-Fatlawi, "Development of 3D Geological Model and Analysis of the Uncertainty in a Tight Oil Reservoir in the Halfaya Oil Field," *The Iraqi Geological Journal*, pp. 128-14, 2, 2023, https://doi.org/10.46717/igj.56.1B.10ms-2023-2-18

[40] A. Rotaru *et al.*, "Horizontal Wells Geosteering and Reservoir Characterization by Using Advanced Mud Logging on the Example of the Terrigenous Reservoir of Eastern Siberia," in *SPE Russian Petroleum Technology Conference?*, 2019: SPE, p. D013S003R006. https://doi.org/10.2118/196960-MS

[41] J. Neal, L. Boatner, Z. Bell, H. Akkurt, and M. McCarthy, "Evaluation of neutron and gamma detectors for high-temperature well-logging applications," in *2011 Future of Instrumentation International Workshop (FIIW) Proceedings*, 2011: IEEE, pp. 172-175, https://doi.org/10.1109/FIIW.2011.6476818

[42] J. A. Jarzyna, S. Baudzis, M. Janowski, and E. Puskarczyk, "Geothermal Resources Recognition and Characterization on the Basis of Well Logging and Petrophysical Laboratory Data, Polish Case Studies," *Energies*, vol. 14, no. 4, p. 850, 2021, https://doi.org/10.3390/en14040850

[43] T. Deng, J. Ambía, and C. Torres-Verdín, "Interpretation of well logs and core data via Bayesian inversion," *Geophysics*, vol. 88, no. 2, pp. D49-D67, 2023, https://doi.org/10.1190/geo2022-0164.1

[44] K. Katterbauer and A. Al Shehri, "A Novel Well Log Data Quality Prescriptive Framework for Enhancing Well Log Data Quality Interpretation," in *Middle East Oil, Gas and Geosciences Show*, 2023: OnePetro, https://doi.org/10.2118/213224-ms

[45] S. Mishra, C. Shrivastava, A. Ojha, and F. Miotti, "Enhancing Reservoir Characterization by Calibrating 3D Reservoir Model with Inter-Well Data in 2D Space," in *SPE Oil and Gas India Conference and Exhibition*, 2019: OnePetro, https://doi.org/10.2118/194607-MS

[46] R. Khisamov *et al.*, "Well logging data interpretation in oil and gas source rock sections based on complex petrophysical and geochemical analysis results," in *SPE Russian Petroleum Technology Conference*, 2018: OnePetro, https://doi.org/10.2118/191675-18RPTC-MS

[47] R. O. Baker, H. W. Yarranton, and J. Jensen, *Practical reservoir engineering and characterization*. Gulf Professional Publishing, 2015.

[48] K. Lehmann, "Environmental corrections to gamma-ray log data: Strategies for geophysical logging with geological and technical drilling," *Journal of applied geophysics*, vol. 70, no. 1, pp. 17-26, 2010, https://doi.org/10.1016/J.JAPPGEO.2009.10.001

[49] A. Buono, S. Fullmer, K. Luck, K. Peterson, P. More, and S. LeBlanc, "Quantitative digital petrography: full thin section quantification of pore space and grains," in *SPE Middle East Oil and Gas Show and Conference*, 2019: OnePetro, https://doi.org/10.2118/194899-MS

[50] V. Krutko *et al.*, "A new approach to clastic rocks pore-scale topology reconstruction based on automatic thin-section images and CT scans analysis," in *SPE Annual Technical Conference and Exhibition*, 2019: OnePetro, https://doi.org/10.2118/196183-MS

[51] M. Abedini, M. Ziaii, and J. Ghiasi-Freez, "The application of Committee machine with particle swarm optimization to the assessment of permeability based on thin section image analysis," *International Journal of Mining and Geo-Engineering*, vol. 52, no. 2, pp. 177-185, 2018, https://doi.org/10.22059/IJMGE.2018.223076.594649

[52] Y. J. Tawfeeq and J. A. Al-Sudani, "Digital Rock Samples Porosity Analysis by OTSU Thresholding Technique Using MATLAB," *Iraqi Journal of Chemical and Petroleum Engineering*, vol. 21, no. 3, pp. 57-66, 2020. https://doi.org/10.31699/IJCPE.2020.3.8

[53] J. Ghiasi-Freez, I. Soleimanpour, A. Kadkhodaie-Ilkhchi, M. Ziaii, M .Sedighi, and A. Hatampour, "Semi-automated porosity identification from thin section images using image analysis and intelligent discriminant classifiers," *Computers & geosciences*, vol. 45, pp. 36-45, 2012, https://doi.org/10.1016/J.CAGEO.2012.03.006

[54] G. Bowers and T. J. Katsube, "AAPG Memoir 76, Chapter 5: The Role of Shale Pore Structure on the Sensitivity of Wire-Line Logs to Overpressure," 2001.

[55] S.-L. Kung, C. Lewis, and J.-C. Wu, "A technique for improving pseudo-synthetic seismograms generated from neutron logs in gas-saturated clastic rocks," *Journal of Geophysics and Engineering*, vol. 10, no. 3, p. 035015, 2013, https://doi.org/10.1088/1742-2132/10/3/035015

[56] T. Darling, *Well logging and formation evaluation*. Elsevier, 2005.

[57] I. Taggart, "Effective versus Total Porosity Based Geostatistical Models: Implications for Upscaling and Flow Simulation," *Transport in Porous Media*, vol. 46, no. 2, pp. 251-268, 2002/02/01 2002, https://doi.org/10.1023/A:1015052712760

[58] L. I. Schlumberger, "vol. II-Applications," *New York*, 1974.

[59] G. B. Asquith, D. Krygowski, and C. R. Gibson, *Basic well log analysis*. American Association of Petroleum Geologists Tulsa, 2004.

[60] B. S. Mulyanto, O. Dewanto, A. Yuliani, A. Yogi, and R. C. Wibowo, "Porosity and permeability prediction using pore geometry structure method on tight carbonate reservoir," in *Journal of Physics: Conference Series*, 2020, vol. 1572, no. 1: IOP Publishing, p. 012052, https://doi.org/10.1088/1742-6596/1572/1/012052

[61] M. Khalid, S. E.-D. Desouky, M. Rashed, T. Shazly, and K. Sediek, "Application of hydraulic flow units' approach for improving reservoir characterization and predicting permeability," *Journal of Petroleum Exploration and Production Technology*, vol. 10, pp. 467-479, 2020, https://doi.org/10.1007/s13202-019-00758-7

[62] H. Al-Ibadi and S. Al-Jawad, "Determination of Flow Units by Integrating Petrophysical Properties of a Giant Middle East Carbonate Reservoir," in *EAGE 2020 Annual Conference & Exhibition Online*, 2020, vol. 2020, no. 1: European Association of Geoscientists & Engineers, pp. 1-5, https://doi.org/10.3997/2214-4609.202011926

[63] S. A. Lazim, S. M. Hamd-Allah, and A. Jawad, "Permeability Estimation for Carbonate Reservoir (Case Study/South Iraqi Field)," *Iraqi Journal of Chemical and Petroleum Engineering*, vol.19 ,no. 3, pp. 41-45, 2018, https://doi.org/10.31699/IJCPE.2018.3.5

[64] A. M. Al-Heeti and O. F. Al-Fatlawi, "Review of Historical Studies for Water Saturation Determination Techniques," *The Iraqi Geological Journal*, pp. 42-62, 2022, https://doi.org/10.46717/igj.55.2A.4Ms-2022-07-20

[65] O. Serra and L. Serra, "Well Logging - Data Acquisition and Applications," ed: Editions Technip.

[66] P. Masoudi, B. Arbab, and H. Mohammadrezaei, "Net pay determination by Dempster rule of combination: Case study on Iranian offshore oil fields," *Journal of Petroleum Science and Engineering*, vol. 123, pp. 78-83, 2014, https://doi.org/10.1016/J.PETROL.2014.07.014

[67] O. Chudi *et al.*, "Integration of Rock Physics and Seismic Inversion for Net-To-Gross Estimation: Implication for Reservoir Modelling and Field Development in Offshore Niger Delta," in *SPE Nigeria Annual International Conference and Exhibition*, 2019: SPE, p. D033S028R010 . https://doi.org/10.2118/198765-MS

[68] J. C. Rivenæs, P. Sørhaug, and R. Knarud, "Introduction to reservoir modelling," *Petroleum Geoscience: From Sedimentary Environments to Rock Physics*, pp. 559-580, 2015, https://doi.org/10.1007/978-3-642-34132-8_22

[69] A. H. Al-maini and E. N. Mad'hat, "Well Log Analysis and Interpretation for Khasib, Tanuma, and Sa'di formations for Halfaya Oil Field in Missan Govenorate-Southern Iraq," *Iraqi Journal of Science*, pp. 520-533, 2018.

استخدام تحليلات سجلات الآبار لحساب الخصائص البتروفيزيائية في خزان كربوني محكم في حقل حلفايا النفطي

صفيه عطاالله جسام [١، *]، عمر الفتلاوي [١، ٢]، و جلال هاكان كانباز [٣]

١ قسم هندسة النفط، كلية الهندسة، جامعة بغداد، بغداد، العراق
٢ مدرسة غربي أستراليا للعلوم والتعدين والهندسة الكيميائية، جامعة كيرتن، استراليا
٣ شركة كليمباتش للاستشارات، ازمير، تركيا

الخلاصة

تعد خزانات الكربونات مصدرًا أساسيًا للهيدروكربونات في جميع أنحاء العالم ، وتلعب خواصها البتروفيزيائية دورًا مهمًا في إنتاج الهيدروكربونات. أهم الخصائص البتروفيزيائية لخزانات الكربونات هي المسامية والنفاذية وتشبع الماء. الخزان المحكم هو خزان ذو مسامية ونفاذية منخفضه، مما يعني أنه من الصعب على السوائل أن تنتقل من جانب إلى آخر. هدف الدراسة هي حساب الخصائص البتروفيزيائية لمكمن السعدي الواقع في حقل حلفايا النفطي الذي يعتبر من أهم حقول النفط في العراق ، ويقع على بعد ٣٥ كم جنوب مدينة العمارة. يتكون تكوين السعدي من أربع وحدات: A، B1، B2 ، وB3 ، تم استبعاد Sadi A لأنها طبقة مائية تفتقر للهيدروكربونات. تم بناء النماذج الهيكلية والبتروفيزيائية بالاعتماد على الداتا المتوفرة من خمسة آبار نفطية. متمثلة بسجلات الآبار من أهمها(RHOB , NPHI ,SONIC, Gamma-Ray , Caliper) وسجلات المقاومة ،من اجل حساب الخصائص البتروفيزيائية. حيث تم تحليل هذه السجلات وتصحيحها للعوامل البيئية باستخدام برنامج IP V3.5. حيث تم تحديد متوسط مقاومة الماء لتكوين السعدي (Rw = 0.04) ، ومتوسط مقاومة ترشيح الطين (Rmf = 0.06) ، ومعلمات Archie (m = 2، n = 1.9 ، و a = 1). وبالتالي تم حساب كل من المسامية والنفاذية وتشبع الماء ونسبة السماكة الصافية إلى الإجمالية (N/G) بناءً على قيم بيانات سجلات الآبار.

الكلمات الدالة: الخصائص البتروفيزيائية، المكامن الكاربونية، تقييم التكوين، FZI.